Chapter 5

EGOE(1+2)-π: Density of States and Parity Ratios

5.1 Introduction

Parity is an important symmetry for finite quantum systems such as nuclei and atoms. In this chapter, we consider EGOE that includes parity explicitly and address three important questions related to parity in nuclear structure. These are as follows:

(i) Parity ratios of nuclear level densities is an important ingredient in nuclear astrophysical applications. Recently, a method based on non-interacting Fermi-gas model for proton-neutron systems has been developed and the parity (π) ratios as a function of excitation energy in large number of nuclei of astrophysical interest have been tabulated [Mo-07]. The method is based on the assumption that the probability to occupy s out of N given sp states follow Poisson distribution in the dilute limit ($m << N, N \rightarrow \infty$ where m is the number of particles). Then the ratio of the partition functions for the +ve and −ve parity states is given by the simple formula $Z_-/Z_+ = \tanh f$, where f is average number of particles in the +ve parity states. Starting with this, an iterative method is developed with inputs from the Fermi-Dirac distribution for occupancies including pairing effects and the Fermi-gas form for the total level density. In the examples studied in [Mo-07], parity ratios are found to equilibrate only around $5-10$ MeV excitation energy. However, ab-initio interacting particle theory for parity

ratios is not yet available.

(ii) A closely related question is about the form of the density of states defined over spaces with fixed-π. In general, fixed-π density of states can be written as a sum of appropriate partial densities. In the situation that the form of the partial densities is determined by a few parameters (as it is with a Gaussian or a Gaussian with one or two corrections), it is possible to derive a theory for these parameters and using these, one can construct fixed-π density of states and calculate parity ratios. Such a theory with interactions in general follows from random matrix theory [Ko-10].

(iii) There is the important recognition in the past few years that random interactions generate regular structures [Ze-04, Zh-04a, Pa-07, Ho-10]. It was shown in [Zh-04] that shell-model for even-even nuclei gives preponderance of +ve parity ground states. A parameter-free EGOE with parity has been defined and analyzed recently by Papenbrock and Weidenmüller [Pa-08] to address the question of 'preponderance of ground states with positive parity' for systems with even number of fermions. They show that in the dilute limit, +ve parity ground states appear with only 50% probability. Thus, a random matrix theory describing shell-model results is not yet available.

With the success of the embedded random matrix ensembles, one can argue that the EE generated by parity preserving random interaction may provide generic results for the three nuclear structure quantities mentioned above. For nuclei, the GOE versions of EE are relevant. Then, with a chaos producing two-body interaction preserving parity in the presence of a mean-field, we have embedded Gaussian orthogonal ensemble of one plus two-body interactions with parity [hereafter called EGOE(1+2)-π]. This model contains two mixing parameters and a gap between the +ve and −ve parity sp states and it goes much beyond the simpler model considered in [Pa-08]. In the random matrix model used in the present chapter, proton-neutron degrees of freedom and angular momentum (J) are not considered. Let us add that in the present chapter for the first time a random matrix theory for parity ratios is attempted. All the results presented in this chapter are published in [Ma-11a].

5.2 EGOE(1+2)-π Ensemble

Given N_+ number of positive parity sp states and similarly N_- number of negative parity sp states, let us assume, for simplicity, that the +ve and −ve parity states are degenerate and separated by energy Δ; see Fig. 5.1. This defines the one-body part $h(1)$ of the Hamiltonian H with $N = N_+ + N_-$ sp states. The matrix for the two-body part $V(2)$ of H [we assume H is (1+2)-body] will be a 3×3 block matrix in two-particle spaces as there are three possible ways to generate two-particle states with definite parity: (i) both fermions in +ve parity states; (ii) both fermions in −ve parity states; (iii) one fermion in +ve and other fermion in −ve parity states. They will give the matrices A, B, and C, respectively in Fig. 5.1. For parity preserving interactions only the states (i) and (ii) will be mixed and mixing matrix is D in Fig. 5.1. Note that the matrices A, B and C are symmetric square matrices while D is in general a rectangular mixing matrix. Consider N sp states arranged such that the states 1 to N_+ have +ve parity and states $N_+ + 1$ to N have −ve parity. Then the operator form of H preserving parity is,

$$
\begin{aligned}
H &= h(1) + V(2)\,; \\
h(1) &= \sum_{i=1}^{N_+} \epsilon_i^{(+)} \hat{n}_i^{(+)} + \sum_{i=N_+ +1}^{N} \epsilon_i^{(-)} \hat{n}_i^{(-)}\,; \quad \epsilon_i^{(+)} = 0\,,\ \epsilon_i^{(-)} = \Delta\,, \\
V(2) &= \sum_{\substack{i,j,k,l=1 \\ (i<j,\ k<\ell)}}^{N_+} \langle \nu_k \nu_\ell \mid V \mid \nu_i \nu_j \rangle\, a_k^\dagger a_\ell^\dagger a_j a_i \\
&+ \sum_{\substack{i',j',k',\ell'=N_+ +1 \\ (i'<j',\ k'<\ell')}}^{N} \langle \nu_{k'} \nu_{\ell'} \mid V \mid \nu_{i'} \nu_{j'} \rangle\, a_{k'}^\dagger a_{\ell'}^\dagger a_{j'} a_{i'} \\
&+ \sum_{i'',k''=1}^{N_+} \sum_{j'',\ell''=N_+ +1}^{N} \langle \nu_{k''} \nu_{\ell''} \mid V \mid \nu_{i''} \nu_{j''} \rangle\, a_{k''}^\dagger a_{\ell''}^\dagger a_{j''} a_{i''}
\end{aligned}
\tag{5.2.1}
$$

$$+ \sum_{\substack{P,Q=1 \\ (P<Q)}}^{N_+} \sum_{\substack{R,S=N_++1 \\ (R<S)}}^{N} \left[\langle \nu_P \nu_Q \mid V \mid \nu_R \nu_S \rangle \, a_P^\dagger \, a_Q^\dagger \, a_S \, a_R + \text{h.c.} \right] .$$

In Eq. (5.2.1), ν_i's are sp states with $i = 1, 2, \ldots, N$ (the first N_+ states are +ve parity and remaining −ve parity). Similarly, $\langle \ldots \mid V \mid \ldots \rangle$ are the two-particle matrix elements, $\hat{n}_i$ are number operators and $a_i^\dagger$ and a_i are creation and annihilation operators, respectively. Note that the four terms in the RHS of the expression for $V(2)$ in Eq. (5.2.1) correspond, respectively, to the matrices A, B, C and D shown in Fig. 5.1.

Many-particle states for m fermions in the N sp states can be obtained by distributing m_1 fermions in the +ve parity sp states (N_+ in number) and similarly, m_2 fermions in the −ve parity sp states (N_- in number) with $m = m_1 + m_2$. Let us denote each distribution of m_1 fermions in N_+ sp states by $\mathbf{m_1}$ and similarly, $\mathbf{m_2}$ for m_2 fermions in N_- sp states. Many-particle basis defined by $(\mathbf{m_1}, \mathbf{m_2})$ with m_2 even will form the basis for +ve parity states and similarly, with m_2 odd for −ve parity states. In the $(\mathbf{m_1}, \mathbf{m_2})$ basis with m_2 even (or odd), the H matrix construction reduces to the matrix construction for spinless fermion systems. The method of construction for spinless fermion systems is well known (see Chapter 1) and therefore it is easy to construct the many-particle H matrices in +ve and −ve parity spaces. The matrix dimensions d_+ for +ve parity and d_- for −ve parity spaces are given by,

$$d_+ = \sum_{m_1, m_2 \, (m_2 \, even)} \binom{N_+}{m_1} \binom{N_-}{m_2}, \quad d_- = \sum_{m_1, m_2 \, (m_2 \, odd)} \binom{N_+}{m_1} \binom{N_-}{m_2}. \tag{5.2.2}$$

Some examples for the dimensions d_+ and d_- are given in Table 5.1.

The EGOE(1+2)-π ensemble is defined by choosing the matrices A, B and C to be independent GOE's with matrix elements variances v_a^2, v_b^2, and v_c^2, respectively. Similarly the matrix elements of the mixing D matrix are chosen to be independent (independent of A, B and C matrix elements) zero centered Gaussian variables with variance v_d^2. Without loss of generality we choose $\Delta = 1$ so that all the v's are in Δ units. This general EGOE(1+2)-π model will have too many parameters $(v_a^2, v_b^2, v_c^2, v_d^2, N_+, N_-, m)$ and therefore it is necessary to reduce the number of parameters. A numerically tractable and physically relevant (as discussed ahead) re-

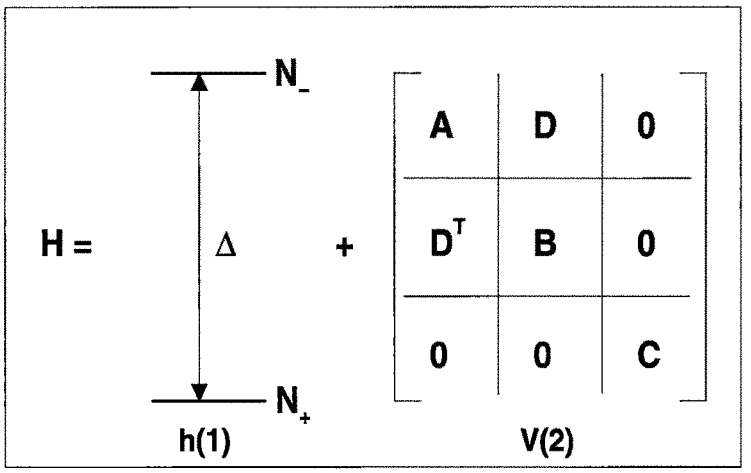

Figure 5.1: Parity preserving one plus two-body H with a sp spectrum defining $h(1)$ along with a schematic form of the $V(2)$ matrix. Dimension of the matrices A, B and C are $N_+(N_+-1)/2$, $N_-(N_--1)/2$, and N_+N_-, respectively. Note that D^T is the transpose of the matrix D. See text for details.

Table 5.1: Hamiltonian matrix dimensions d_+ and d_- for various values of (N_+, N_-, m).

N_+	N_-	m	d_+	d_-	N_+	N_-	m	d_+	d_-
6	6	6	452	472	8	8	4	924	896
7	5	6	462	462			5	2184	2184
7	7	5	1001	1001			6	3976	4032
		6	1484	1519	10	6	4	900	920
		7	1716	1716			5	2202	2166
8	6	5	1016	986			6	4036	3972
		6	1499	1504	6	10	4	900	920
9	5	5	1011	911			5	2166	2202
		6	1524	1479			6	4036	3972
5	10	4	665	700	9	9	6	9240	9324
		5	1501	1502	10	8	6	9268	9296
					10	10	5	7752	7752
							6	19320	19440

striction is to choose the matrix elements variances of the diagonal blocks A, B and C to be same and then we have the EGOE(1+2)-π model defined by (N_+, N_-, m) and the variance parameters (τ,α) where

$$\frac{v_a^2}{\Delta^2} = \frac{v_b^2}{\Delta^2} = \frac{v_c^2}{\Delta^2} = \tau^2\,, \quad \frac{v_d^2}{\Delta^2} = \alpha^2\,. \tag{5.2.3}$$

Thus EGOE(1+2)-π we employ is

$$\begin{aligned} &A\text{: GOE}(0:\tau^2)\,,\ B\text{: GOE}(0:\tau^2)\,,\ C\text{: GOE}(0:\tau^2)\,,\ D\text{: GOE}(0:\alpha^2)\,; \\ &A,\ B,\ C,\ D \text{ are independent GOE's}\,. \end{aligned} \tag{5.2.4}$$

Note that the D matrix is a GOE only in the sense that the matrix elements D_{ij} are all independent zero centered Gaussian variables with variance α^2. In the limit $\tau^2 \to \infty$ and $\alpha = \tau$, the model defined by Eqs. (5.2.1), (5.2.3) and (5.2.4) reduces to the simpler model analyzed in [Pa-08].

Starting with the EGOE(1+2)-π ensemble defined by Eqs. (5.2.1), (5.2.3) and (5.2.4), we have numerically constructed the ensemble in many-particle +ve and −ve parity spaces with dimensions d_+ and d_- given by Eq. (5.2.2) for several values of (N_+, N_-, m) and varying the parameters τ and α. Before discussing the results of the numerical calculations, we present the results for the energy centroids, variances and also the shape parameters (skewness and excess) defining the normalized fixed-(m_1, m_2) partial densities $\rho^{m_1,m_2}(E) = \langle\delta(H-E)\rangle^{m_1,m_2}$. These will allow us to understand some of the numerical results. Let us add that the fixed-π eigenvalue densities $I_\pm(E)$ are sum of the appropriate partial densities as given by Eq. (5.4.4) ahead. Note that the densities $I_\pm(E)$ are normalized to $d_\pm$.

5.3 Energy Centroids, Variances, Skewness and Excess Parameters for Fixed-(m_1, m_2) Partial Densities

Let us call the set of +ve parity sp states as unitary orbit #1 and similarly the set of −ve parity sp states as unitary orbit #2; unitary orbits notation and their significance was discussed in [Ko-10]. For convenience, from now on, we denote the sp states by the roman letters $(i, j, \ldots)$ and unitary orbits by greek letters $(\alpha, \beta, \ldots)$. Note that $\alpha = 1$ corresponds to the +ve parity unitary orbit and $\alpha = 2$ corresponds to the −ve parity unitary orbit (with this notation, $N_1 = N_+$ and $N_2 = N_-$). The sp states that belong to a unitary orbit α are denoted as $i_\alpha, j_\alpha, \ldots$. Propagation formulas for the energy centroids and variances of the partial densities $\rho^{m_1,m_2}(E)$ follow from the unitary decomposition of $V(2)$ with respect to the sub-algebra $U(N_+) \oplus U(N_-)$ contained in $U(N)$. The operator $V(2)$ decomposes into three parts $V(2) \to V^{[0]} + V^{[1]} + V^{[2]}$.

The $V^{[0]}$ generates the energy centroids $\langle V\rangle^{m_1,m_2}$, $V^{[1]}$ corresponds to the 'algebraic' mean-field generated by V and $V^{[2]}$ is the remaining irreducible two-body part. Extending the unitary decomposition for the situation with a single orbit for spinless fermions (see Appendix A) and also using the detailed formulation given in [Ch-71], we obtain the following formulas for the $V^{[\nu]}$'s. The $V^{[0]}$ is given by (with $\alpha = 1, 2$ and $\beta = 1, 2$)

$$
\begin{aligned}
V^{[0]} &= \sum_{\alpha\geq\beta} \frac{\hat{n}_\alpha(\hat{n}_\beta - \delta_{\alpha\beta})}{(1+\delta_{\alpha\beta})} V_{\alpha\beta}\,; \\
V_{\alpha\alpha} &= \binom{N_\alpha}{2}^{-1} \sum_{i>j} V_{i_\alpha j_\alpha i_\alpha j_\alpha}\,, \\
V_{\alpha\beta} &= (N_\alpha N_\beta)^{-1} \sum_{i,j} V_{i_\alpha j_\beta i_\alpha j_\beta}\,; \quad \alpha \neq \beta\,.
\end{aligned}
\tag{5.3.1}
$$

Then the traceless part $\widetilde{V}$ is given by

$$
\begin{aligned}
\widetilde{V} &= V - V^{[0]} = V^{[1]} + V^{[2]}\,; \\
(\widetilde{V})_{i_\alpha j_\beta i_\alpha j_\beta} &= V_{i_\alpha j_\beta i_\alpha j_\beta} - V_{\alpha\beta}\,, \\
(\widetilde{V})_{ijk\ell} &= V_{ijk\ell} \quad \text{for all others}\,.
\end{aligned}
\tag{5.3.2}
$$

Now the $V^{[1]}$ part is

$$
\begin{aligned}
V^{[1]} &= \sum_{i_\alpha, j_\alpha} \widehat{\xi}_{i_\alpha j_\alpha} a^\dagger_{i_\alpha} a_{j_\alpha}\,; \\
\widehat{\xi}_{i_\alpha j_\alpha} &= \sum_\beta \frac{\hat{n}_\beta - \delta_{\alpha\beta}}{N_\beta - 2\delta_{\alpha\beta}} \zeta_{i_\alpha j_\alpha}(\beta)\,, \quad \zeta_{i_\alpha j_\alpha}(\beta) = \sum_{k_\beta} \widetilde{V}_{k_\beta i_\alpha k_\beta j_\alpha}\,.
\end{aligned}
\tag{5.3.3}
$$

It is important to stress that, with spherical (j) orbits and no radial degeneracy (as used in many nuclear structure studies), $V^{[1]}$ part will not exist. Finally, the $V^{[2]}$ part

is as follows,

$$
\begin{aligned}
V^{[2]} &= \widetilde{V} - V^{[1]}\,; \\
V^{[2]}_{i_\alpha j_\beta i_\alpha j_\beta} &= \widetilde{V}_{i_\alpha j_\beta i_\alpha j_\beta} - \left[\frac{\zeta_{i_\alpha j_\alpha}(\beta)}{N_\beta - 2\delta_{\alpha\beta}} + \frac{\zeta_{i_\beta j_\beta}(\alpha)}{N_\alpha - 2\delta_{\alpha\beta}}\right], \\
V^{[2]}_{k_\alpha i_\beta k_\alpha j_\beta} &= \widetilde{V}_{k_\alpha i_\beta k_\alpha j_\beta} - \frac{\zeta_{i_\beta j_\beta}(\alpha)}{N_\alpha - 2\delta_{\alpha\beta}}\,; \quad i_\beta \neq j_\beta\,, \\
V^{[2]}_{ijk\ell} &= \widetilde{V}_{ijk\ell} \text{ for all others}.
\end{aligned}
\tag{5.3.4}
$$

Given the $U(N) \supset U(N_+) \oplus U(N_-)$ unitary (tensorial) decomposition, by intuition and using Eq. (A3), it is possible to write the propagation formulas for the energy centroids and variances of $\rho^{m_1,m_2}(E)$. Note that these are essentially traces of H and H^2 over the space defined by the two-orbit configurations (m_1, m_2); see Eqs. (5.3.5) and (5.3.6) ahead. A direct approach to write the propagation formulas for centroids and variances for a multi-orbit configuration was given in detail first by French and Ratcliff [Fr-71]. The formula for the variance given in [Fr-71] is cumbersome and it is realized later [Ch-71] that they can be made compact by applying group theory (see also [Ko-01, Wo-86, Ko-10]). We have adopted the group theoretical approach for the two-orbit averages and obtained formulas. Propagation formula for the fixed-(m_1, m_2) energy centroids is,

$$
E_c(m_1, m_2) = \langle H \rangle^{m_1,m_2} = m_2\,\Delta + \sum_{\alpha \geq \beta} \frac{m_\alpha (m_\beta - \delta_{\alpha\beta})}{(1 + \delta_{\alpha\beta})}\, V_{\alpha\beta}\,. \tag{5.3.5}
$$

First term in Eq. (5.3.5) is generated by $h(1)$ and is simple because of the choice of the sp energies as shown in Fig. 5.1. Propagation formula for fixed-(m_1, m_2) variances is,

$$
\begin{aligned}
\sigma^2(m_1, m_2) &= \left\langle H^2 \right\rangle^{m_1,m_2} - [\langle H \rangle^{m_1,m_2}]^2 \\
&= \sum_\alpha \frac{m_\alpha\,(N_\alpha - m_\alpha)}{N_\alpha\,(N_\alpha - 1)} \sum_{i_\alpha, j_\alpha} [\xi_{i_\alpha, j_\alpha}(m_1, m_2)]^2
\end{aligned}
\tag{5.3.6}
$$

$$+ \sum_{\alpha,\beta,\gamma,\delta}{}' \frac{m_\alpha(m_\beta-\delta_{\alpha\beta})(N_\gamma-m_\gamma)(N_\delta-m_\delta-\delta_{\gamma\delta})}{N_\alpha(N_\beta-\delta_{\alpha\beta})(N_\gamma-\delta_{\gamma\alpha}-\delta_{\gamma\beta})(N_\delta-\delta_{\delta\alpha}-\delta_{\delta\beta}-\delta_{\delta\gamma})}\,(X)\,;$$

$$\xi_{i_\alpha,j_\alpha}(m_1,m_2)=\sum_\beta \frac{m_\beta-\delta_{\alpha\beta}}{N_\beta-2\delta_{\alpha\beta}}\zeta_{i_\alpha j_\alpha}(\beta)\,,\quad X=\sum{}'\left(V^{[2]}_{i_\alpha j_\beta k_\gamma \ell_\delta}\right)^2\,.$$

The 'prime' over summations in Eq. (5.3.6) implies that the summations are not free sums. Note that $(\alpha,\beta,\gamma,\delta)$ take values (1,1,1,1), (2,2,2,2), (1,2,1,2), (1,1,2,2) and (2,2,1,1). Similarly, in the sum over (i_α, j_β), $i \le j$ if $\alpha=\beta$ and otherwise the sum is over all i and j. Similarly, for (k_γ,ℓ_δ). Using $E_c(m_1,m_2)$ and $\sigma^2(m_1,m_2)$, the fixed-parity energy centroids and spectral variances [they define $I_\pm(E)$] can be obtained as follows,

$$E_c(m,\pm)=\langle H\rangle^{m,\pm}=\frac{1}{d_\pm}\sum_{m_1,m_2}{}' d(m_1,m_2)E_c(m_1,m_2)\,,$$

$$\sigma^2(m,\pm)=\left\langle H^2\right\rangle^{m,\pm}-\left[\langle H\rangle^{m,\pm}\right]^2\,; \tag{5.3.7}$$

$$\left\langle H^2\right\rangle^{m,\pm}=\frac{1}{d_\pm}\sum_{m_1,m_2}{}' d(m_1,m_2)\left[\sigma^2(m_1,m_2)+E_c^2(m_1,m_2)\right]\,.$$

The 'prime' over summations in Eq. (5.3.7) implies that m_2 is even(odd) for +ve(−ve) parity.

It should be pointed out that the formulas given by Eqs. (5.3.5), (5.3.6) and (5.3.7) are compact and easy to understand compared to Eqs. (10)-(14) of [Pa-08] and also those that follow from Eqs. (129) and (133) of [Fr-71] where unitary decomposition is not employed. We have verified Eqs. (5.3.5) and (5.3.6) by explicit construction of the H matrices in many examples. In principle, it is possible to obtain a formula for the ensemble averaged variances using Eq. (5.3.6); the ensemble averaged centroids derive only from $h(1)$. Simple asymptotic formulas for ensemble averaged variances follow by neglecting the δ-functions that appear in Eq. (5.3.6) and replacing $(V^{[2]}_{ijk\ell})^2$ by τ^2 and α^2 appropriately. Then the final formula for the ensemble averaged fixed-

(m_1, m_2) variances is,

$$\overline{\sigma^2(m_1,m_2)} \approx m\left[\sum_{\alpha=1}^{2} m_\alpha (N_\alpha - m_\alpha)\right]\tau^2 + \left[\binom{m_1}{2}\binom{\tilde{m}_2}{2} + \binom{m_2}{2}\binom{\tilde{m}_1}{2}\right]\alpha^2 + \left[\binom{m_1}{2}\binom{\tilde{m}_1}{2} + \binom{m_2}{2}\binom{\tilde{m}_2}{2} + m_1 m_2 \tilde{m}_1 \tilde{m}_2\right]\tau^2 . \tag{5.3.8}$$

Here, $\tilde{m}_1 = N_1 - m_1$ and $\tilde{m}_2 = N_2 - m_2$. In Table 5.2, we compare the results obtained from Eq. (5.3.8) with those obtained for various 100 member ensembles using Eq. (5.3.6) and the agreements are quite good. Therefore, in many practical applications, one can use Eq. (5.3.8).

In practice, fixed-π state densities are constructed as a sum of the partial densities $\rho^{m_1,m_2}(E)$ as discussed in Sec. 5.4.1 ahead. Going beyond the first two moments $M_1(m_1,m_2) = \langle H \rangle^{m_1,m_2}$ and $M_2(m_1,m_2) = \langle H^2 \rangle^{m_1,m_2}$, it is possible to consider the third and fourth moments $M_3(m_1,m_2) = \langle H^3 \rangle^{m_1,m_2}$ and $M_4(m_1,m_2) = \langle H^4 \rangle^{m_1,m_2}$ respectively of $\rho^{m_1,m_2}(E)$. The skewness and excess parameters $\gamma_1(m_1,m_2)$ and $\gamma_2(m_1,m_2)$ give information about the shape of the partial densities and they are close to zero implies Gaussian form. The partial densities $\rho^{m_1,m_2}(E)$ determine the total +ve and −ve parity state densities $I_\pm(E)$; see Eq. (5.4.4) ahead. By extending the binary correlation approximation to evaluate averages over two-orbit configurations, we have derived formulas for $\gamma_1(m_1,m_2)$ and $\gamma_2(m_1,m_2)$. All the details are discussed in Chapter 7. Exact results for skewness $\gamma_1(m,\pm)$ and excess $\gamma_2(m,\pm)$ parameters for fixed-π eigenvalue densities $I_\pm(E)$ are compared with the binary correlation results in Table 7.1 and it is clearly seen from the results in Table 7.1 that in all the examples considered, the binary correlation results are quite close to the exact results. In addition, the following results are inferred from the results in Chapter 7.

It is seen from Eq. (7.2.19), $\gamma_1(m_1,m_2)$ will be non-zero only when $\alpha \neq 0$ and the τ dependence is weak. Also, it is seen that for $N_+ = N_-$, $\gamma_1(m_1,m_2) = -\gamma_1(m_2,m_1)$. Similarly, Eq. (7.2.20) shows that for $N_+ = N_-$, $\gamma_2(m_1,m_2) = \gamma_2(m_2,m_1)$. In the dilute limit, with some approximations as discussed after Eq. (7.2.20), the expression for $\gamma_2(m_2,m_1)$ is given by Eq. (7.2.21). This shows that, for $\alpha << \tau$, $\gamma_2(m_2,m_1) = C_1/[\overline{\langle X^2 \rangle^{m_1,m_2}}]^2$ with $C_1 \sim -9\tau^4 N^4 m^3/16$ for $m_1 = m_2 = m/2$ and $N_1 = N_2 = N$. Eval-

Table 5.2: Ensemble averaged fixed-(m_1, m_2) widths $\sigma(m_1, m_2)$ and the total spectral width σ_t for different (τ, α) values. For each (τ, α), the $\sigma(m_1, m_2)$ are given in the table and they are obtained using the exact propagation formula Eq. (5.3.6) for each member of the ensemble. In all the calculations, 100 member ensembles are employed. Numbers in the bracket are obtained by using the asymptotic formula given in Eq. (5.3.8). Last row for each (N_+, N_-) gives the corresponding σ_t values. All the results are given for 6 particle systems and the dimensions $d(m_1, m_2)$ are also given in the table. See text for details.

				$(\tau, \alpha/\tau)$			
(N_+, N_-)	m_1	m_2	$d(m_1, m_2)$	(0.1, 0.5)	(0.1, 1.5)	(0.2, 0.5)	(0.2, 1.5)
(8,8)	0	6	28	1.36(1.39)	3.21(3.21)	2.73(2.77)	6.41(6.42)
	1	5	448	1.76(1.79)	2.70(2.72)	3.52(3.57)	5.41(5.44)
	2	4	1960	2.05(2.09)	2.48(2.50)	4.11(4.17)	4.96(5.01)
	3	3	3136	2.16(2.19)	2.42(2.45)	4.31(4.38)	4.84(4.90)
	4	2	1960	2.05(2.09)	2.48(2.50)	4.11(4.17)	4.95(5.01)
	5	1	448	1.76(1.79)	2.70(2.72)	3.52(3.57)	5.41(5.44)
	6	0	28	1.37(1.39)	3.21(3.21)	2.75(2.77)	6.42(6.42)
				2.29(2.32)	2.68(2.71)	4.24(4.30)	5.08(5.13)
(6,10)	0	6	210	1.67(1.70)	2.70(2.72)	3.34(3.41)	5.41(5.44)
	1	5	1512	2.04(2.07)	2.48(2.51)	4.08(4.15)	4.97(5.02)
	2	4	3150	2.19(2.22)	2.41(2.44)	4.37(4.44)	4.82(4.88)
	3	3	2400	2.11(2.14)	2.43(2.46)	4.22(4.28)	4.86(4.91)
	4	2	675	1.84(1.87)	2.60(2.62)	3.67(3.73)	5.20(5.24)
	5	1	60	1.46(1.48)	3.06(3.06)	2.92(2.96)	6.12(6.13)
	6	0	1	1.30(1.30)	3.90(3.90)	2.60(2.60)	7.81(7.79)
				2.31(2.33)	2.65(2.67)	4.30(4.36)	5.02(5.07)
(10,10)	0	6	210	1.97(2.01)	4.16(4.19)	3.95(4.01)	8.33(8.37)
	1	5	2520	2.44(2.49)	3.63(3.66)	4.90(4.98)	7.25(7.32)
	2	4	9450	2.76(2.81)	3.36(3.40)	5.53(5.61)	6.71(6.79)
	3	3	14400	2.87(2.92)	3.28(3.32)	5.74(5.83)	6.56(6.64)
	4	2	9450	2.76(2.81)	3.36(3.40)	5.53(5.61)	6.71(6.79)
	5	1	2520	2.44(2.49)	3.63(3.66)	4.90(4.98)	7.25(7.32)
	6	0	210	1.97(2.01)	4.16(4.19)	3.95(4.01)	8.33(8.37)
				2.95(2.99)	3.54(3.57)	5.62(5.70)	6.83(6.91)

uating $\overline{\langle X^2 \rangle^{m_1,m_2}}$ in the dilute limit then gives $\gamma_2 \sim -4/m$. Similarly, for $\tau << \alpha$, we have $\gamma_2(m_2, m_1) = C_2/[\overline{\langle D\tilde{D} \rangle^{m_1,m_2}} + \overline{\langle \tilde{D}D \rangle^{m_1,m_2}}]^2$ with $C_2 \sim -\alpha^4 N^4 m^3/16$ and this gives $\gamma_2 \sim -4/m$. Therefore, in the $\tau << \alpha$ and $\tau >> \alpha$ limit, the result for γ_2 is same as the result for spinless fermion EGOE(2) [Mo-73, Mo-75] and this shows that for a range of (τ, α) values, $\rho^{m_1,m_2}(E)$ will be close to Gaussian. Moreover, to the extent that Eq. (7.2.21) applies, the density $\rho^{m_1,m_2}(E)$ is a convolution of the densities generated

by $X(2)$ and $D(2)$ operators. Let us add that the binary correlation results presented in Chapter 7, with further extensions, will be useful in the study of partitioned EGOE discussed in [Ko-01, Ko-99]. Now we present some numerical results.

5.4 Numerical Results and Discussion

In order to proceed with the calculations, we need to have some idea of the range of the parameters $(\tau, \alpha, m/N_+, N_+/N_-)$. Towards this end, we have used realistic nuclear effective interactions in $sdfp$ [No-09] and $fpg_{9/2}$ [So-02] spaces and calculated the variances v_a^2, v_b^2, v_c^2, v_d^2 for these interactions. Note that it is easy to identify the matrices A, B, C and D given the interaction matrix elements $\langle (j_1 j_2) JT \mid V \mid (j_3 j_4) JT \rangle$. To calculate the mean-squared matrix elements v^2's, we put the diagonal two-particle matrix elements to be zero and use the weight factor $(2J+1)(2T+1)$. Assuming that $\Delta = 3$ MeV and 5 MeV (these are reasonable values for $A = 20-80$ nuclei), we obtain $\tau \sim 0.09 - 0.24$ and $\alpha \sim (0.9-1.3) \times \tau$. These deduced values of α and τ clearly point out that one has to go beyond the highly restricted ensemble employed in [Pa-08] and it is necessary to consider the more general EGOE(1+2)-π defined in Sec. 5.2. Similarly, for $sdfp$ and $fpg_{9/2}$ spaces $N_+/N_- \sim 0.5-2.0$. Finally, for nuclei with m number of valence nucleons (particles or holes) where $sdfp$ or $fpg_{9/2}$ spaces are appropriate, usually $m \lesssim N_+$ or N_-, whichever is lower. Given these, we have selected the following examples: (N_+, N_-, m) = (8,8,4), (8,8,5), (10,6,4), (10,6,5), (6,10,4), (6,10,5), (8,8,6), (6,6,6), (7,7,7) and (7,7,6). To go beyond the matrix dimensions $\sim$ 5000 with 100 members is not feasible at present with the HPC cluster that is used for all the calculations. Most of the discussion in this chapter is restricted to $N = N_+ + N_- = 16$ and $m << N$ as in this dilute limit, it is possible to understand the ensemble results better. Following the nuclear examples mentioned above, we have chosen τ = 0.05, 0.1, 0.2, 0.3 and α/τ = 0.5, 1.0, 1.5. We will make some comments on the results for other (τ, α) values at appropriate places.

Now we will present the results for (i) the form of the +ve and −ve parity state densities $I_+(E)$ and $I_-(E)$, respectively, (ii) the parity ratios $I_-(E)/I_+(E)$ vs E where E is the excitation energy of the system and (iii) the probability for +ve parity ground states generated by the EGOE(1+2)-π ensemble.

5.4.1 Gaussian form for fixed-π state densities

Using the method discussed in Sec. 5.2, we have numerically constructed in +ve and −ve parity spaces EGOE(1+2)-π ensembles of random matrices consisting of 100 Hamiltonian matrices in large number of examples, i.e. for (N_+, N_-, m) and (τ, α) parameters mentioned above. Diagonalizing these matrices, ensemble averaged eigenvalue (state) densities,

$$\overline{I_\pm(E)} = \overline{\langle\langle \delta(H-E)\rangle\rangle^\pm}\,, \tag{5.4.1}$$

are constructed. From now on, we drop the "overline" symbol when there is no confusion. Results are shown for $(N_+, N_-, m) = (8,8,4)$, $(8,8,5)$, $(10,6,5)$ and $(6,10,5)$ for several values of (τ, α) in Figs. 5.2, 5.3 and 5.4. To construct the fixed-parity eigenvalue densities, we first make the centroids $E_c(m,\pm)$ of all the members of the ensemble to be zero and variances $\sigma^2(m,\pm)$ to be unity, i.e., for each member we have the standardized eigenvalues $\widehat{E} = [E - E_c(m,\pm)]/\sigma(m,\pm)$. Then, combining all the $\widehat{E}$ and using a bin-size $\Delta\widehat{E} = 0.2$, histograms for $I_\pm(E)$ are generated. It is seen that the state densities are multimodal for small τ values and for $\tau \geq 0.1$, they are unimodal and close to a Gaussian. Note that in our examples, $\alpha = (0.5 - 1.5) \times \tau$.

For $V(2) = 0$, the eigenvalue densities will be a sum of spikes at 0, 2Δ, 4Δ, ... for +ve parity densities and similarly at Δ, 3Δ, 5Δ, ... for −ve parity densities. As we switch on $V(2)$, the spikes will spread due to the matrices A, B and C in Fig. 5.1 and mix due to the matrix D. The variance $\sigma^2(m_1, m_2)$ can be written as,

$$\sigma^2(m_1, m_2) = \sigma^2(m_1, m_2 \rightarrow m_1, m_2) + \sigma^2(m_1, m_2 \rightarrow m_1 \pm 2, m_2 \mp 2)\,. \tag{5.4.2}$$

The internal variance $\sigma^2(m_1, m_2 \rightarrow m_1, m_2)$ is due to A, B and C matrices and it receives contribution only from the τ parameter. Similarly, the external variance $\sigma^2(m_1, m_2 \rightarrow m_1 \pm 2, m_2 \mp 2)$ is due to the matrix D and it receives contribution only from the α parameter. When we switch on $V(2)$, as the ensemble averaged centroids generated by $V(2)$ will be zero, the positions of the spikes will be largely unaltered. However, they will start spreading and mixing as τ and α increase. Therefore, the density will be multimodal with the modes well separated for very small (τ, α) values. Some examples for this are shown in Fig. 5.5. As τ and α start increasing from zero,

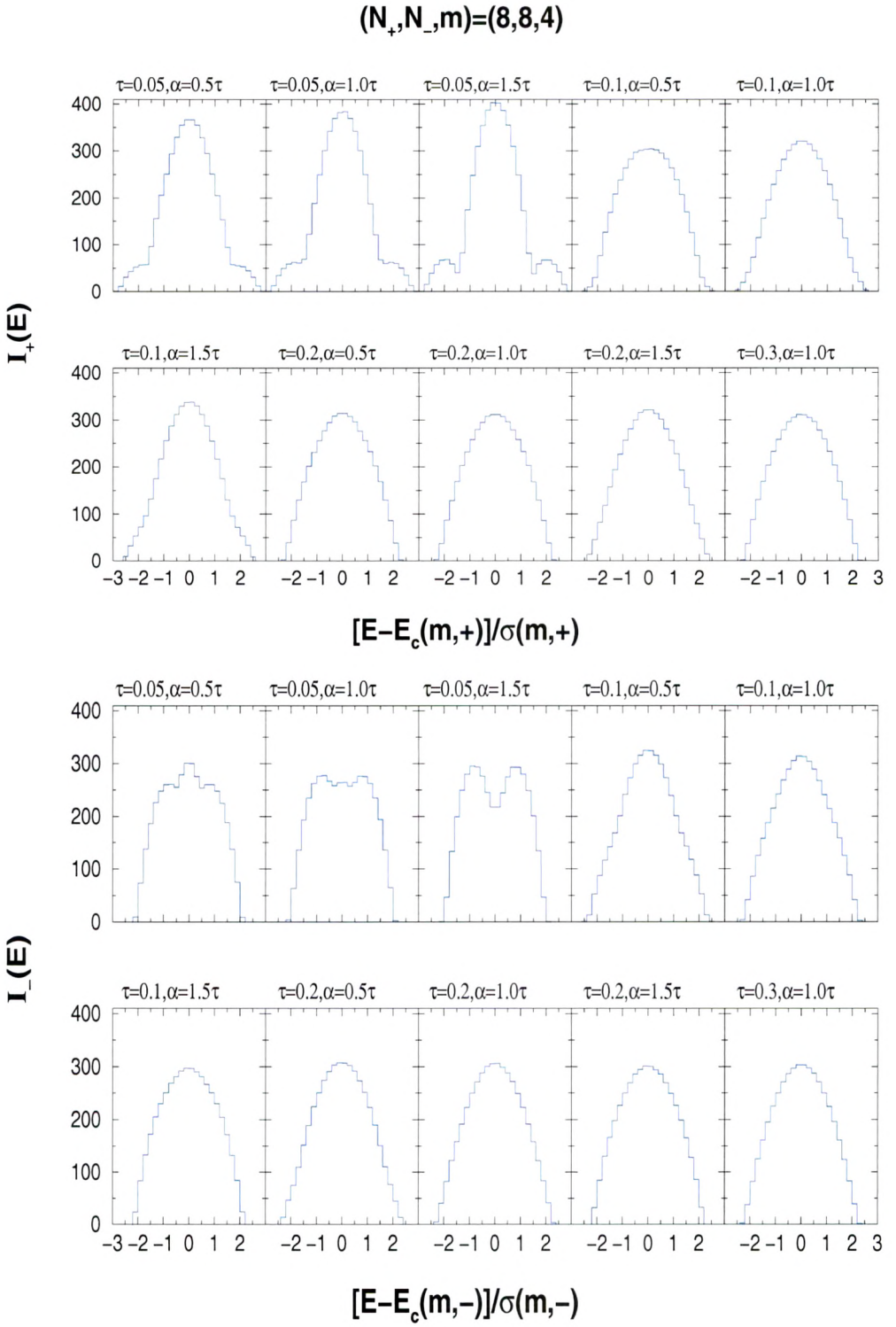

Figure 5.2: Positive and negative parity state densities for various (τ, α) values for $(N_+, N_-, m) = (8, 8, 4)$ system. See text for details.

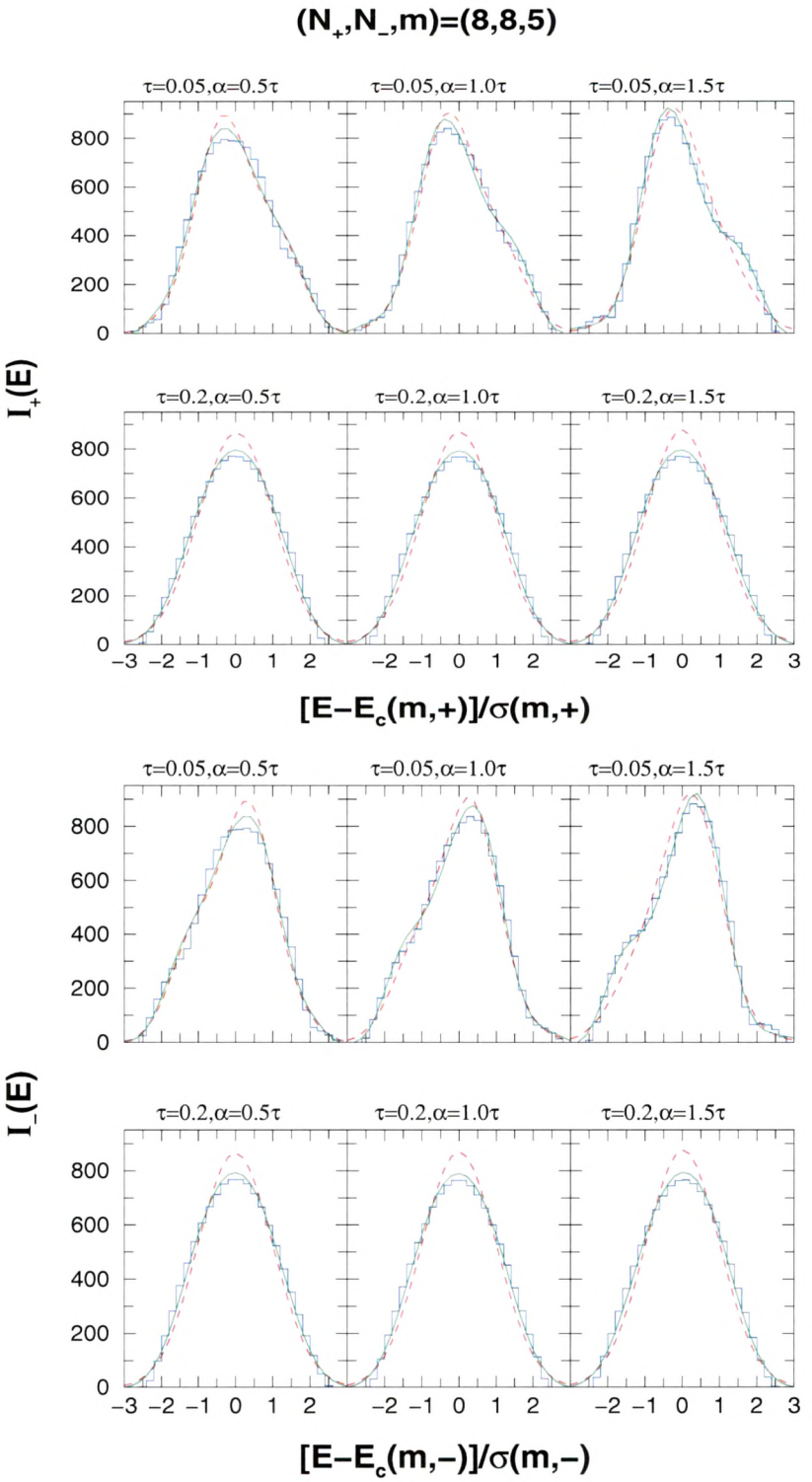

Figure 5.3: Positive and negative parity state densities for various (τ, α) values for $(N_+, N_-, m) = (8, 8, 5)$ system. Histograms are numerical ensemble results. The dashed (red) curve corresponds to Gaussian form for $\rho^{m_1,m_2}(E)$ in Eq. (5.4.4) and similarly, solid (green) curve corresponds to Edgeworth corrected Gaussian form with $\gamma_1(m_1, m_2)$ and $\gamma_2(m_1, m_2)$ obtained using the results in Chapter 7. See text for details.

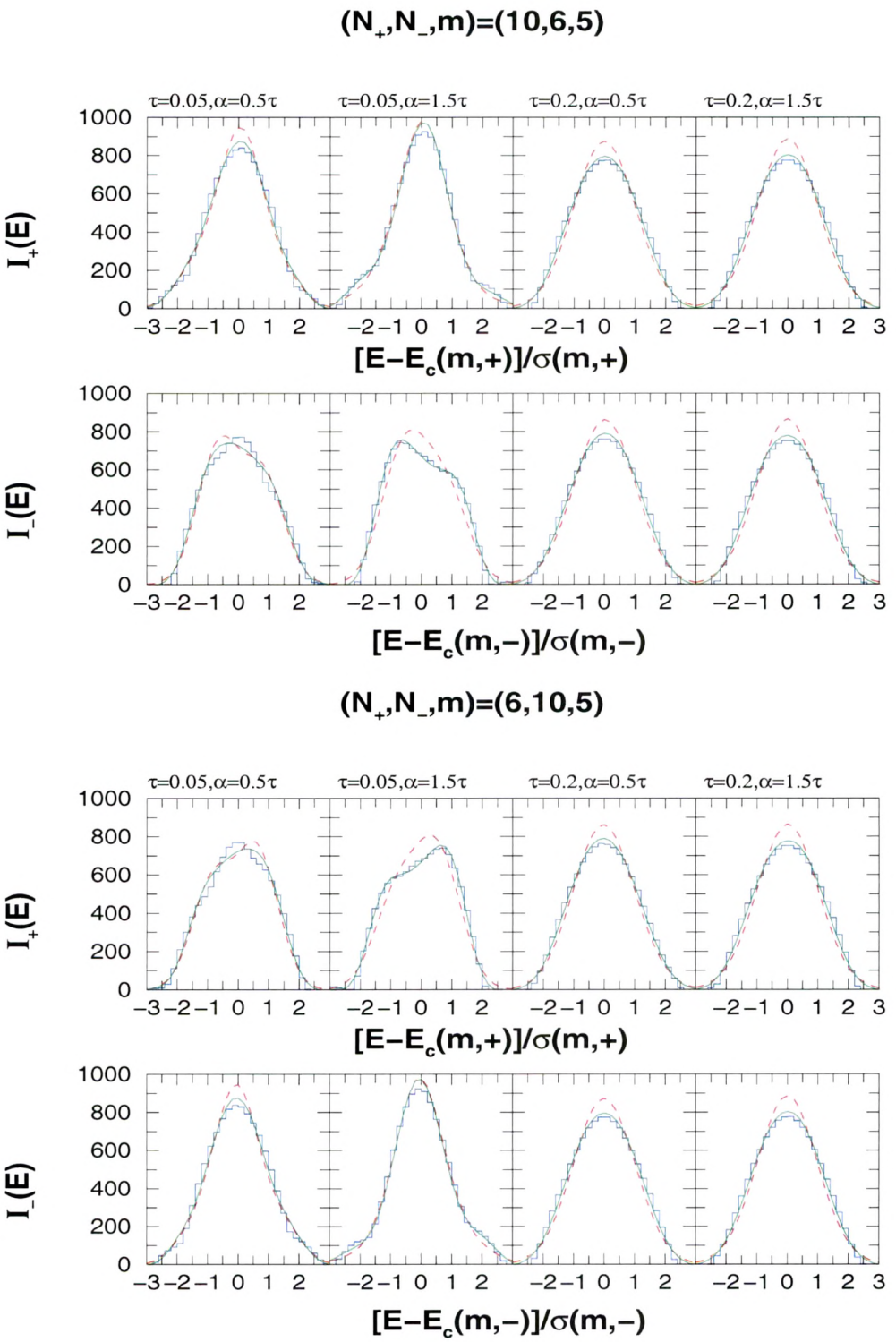

Figure 5.4: Positive and negative parity state densities for various (τ, α) values for $(N_+, N_-, m) = (10, 6, 5)$ and $(6, 10, 5)$ systems. Histograms are numerical ensemble results. The dashed (red) curve corresponds to Gaussian form for $\rho^{m_1,m_2}(E)$ in Eq. (5.4.4) and similarly, solid (green) curve corresponds to Edgeworth corrected Gaussian form with $\gamma_1(m_1, m_2)$ and $\gamma_2(m_1, m_2)$ obtained using the results in Chapter 7. See text for details.

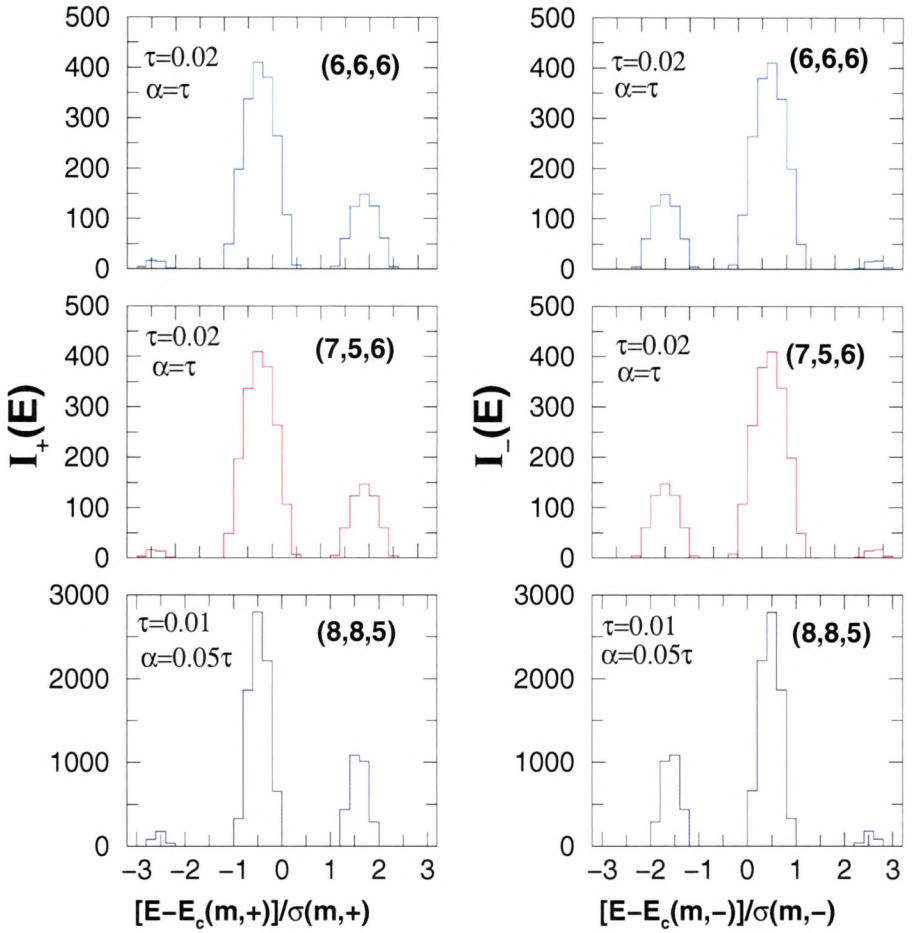

Figure 5.5: Positive and negative parity state densities for some small values of (τ, α). The (N_+, N_-, m) values are given in the figures. See text for details.

the spikes spread and will start overlapping for $\sigma(m_1, m_2) \gtrsim \Delta$. This is the situation with $\tau = 0.05$ shown in Figs. 5.2, 5.3 and 5.4. However, as τ increases (with $\alpha \sim \tau$), the densities start becoming unimodal as seen from the $\tau = 0.1$ and 0.2 examples. Also, the m dependence is not strong as seen from the Figs. 5.2, 5.3 and 5.4. Now we will discuss the comparison of the ensemble results with the smoothed densities constructed using $E_c(m_1, m_2)$, $\sigma^2(m_1, m_2)$, $\gamma_1(m_1, m_2)$ and $\gamma_2(m_1, m_2)$.

As the particle numbers in the examples shown in Figs. 5.2, 5.3 and 5.4 are small, the excess parameter $\gamma_2^\pi(m) \sim -0.7$ to -0.8 (skewness parameter $\gamma_1^\pi(m) \sim 0$ in all our examples). Therefore the densities are not very close to a Gaussian form. It has been well established that the ensemble averaged eigenvalue density takes Gaussian form in the case of spinless fermion (as well as boson) systems and also for the embedded ensembles extending to those with good quantum numbers; see Chapter 2

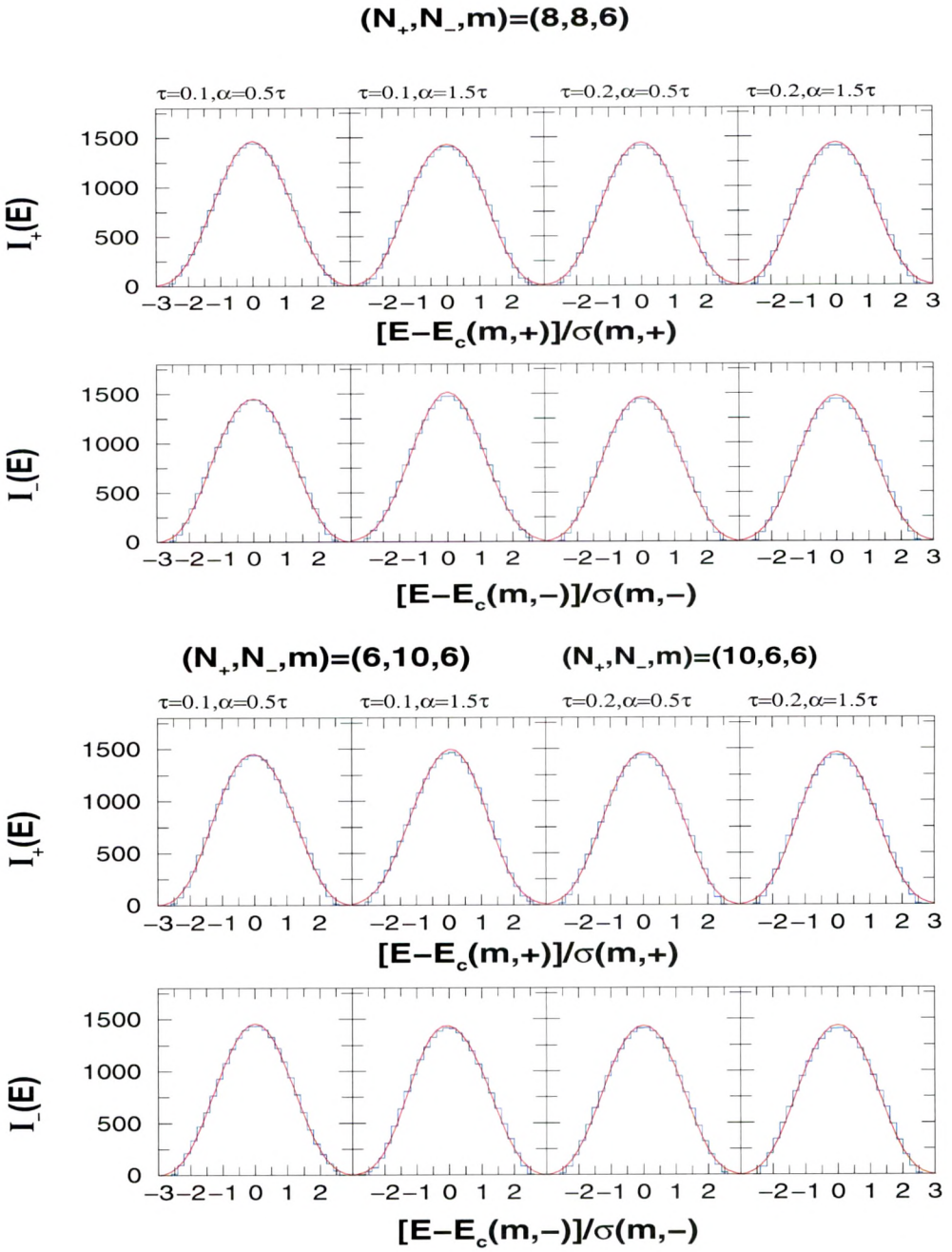

Figure 5.6: Positive and negative parity state densities for various (τ, α) values for $(N_+, N_-, m) = (8,8,6)$, $(6,10,6)$ and $(10,6,6)$ systems. Smoothed curves (solid red lines) are obtained using fixed-(m_1, m_2) partial densities. See text for details.

and [Ko-01, Go-11]. Thus, it can be anticipated that Gaussian form is generic for the state densities or more appropriately, for the partial densities $\rho^{m_1,m_2}(E)$ generated by EGOE(1+2)-π for sufficiently large values of (τ, α). Results for the fixed-π densities for $(N_+, N_-, m) = (8,8,6)$, $(6,10,6)$ and $(10,6,6)$ systems are shown in Fig. 5.6. The

smoothed +ve and −ve parity densities are a sum of the partial densities $\rho^{m_1,m_2}(E)$,

$$\rho_{\pm}(E) = \frac{1}{d_{\pm}} \sum_{m_1,m_2}^{\prime} d(m_1,m_2)\rho^{m_1,m_2}(E)\,. \tag{5.4.3}$$

Note that the summation in Eq. (5.4.3) is over m_2 even for +ve parity density and similarly over m_2 odd for −ve parity density. Here $\rho_{\pm}(E)$ as well as $\rho^{m_1,m_2}(E)$ are normalized to unity. However, in practice, the densities normalized to dimensions are needed and they are denoted, as used earlier, by $I_{\pm}(E)$ and $I^{m_1,m_2}(E)$, respectively,

$$I_{\pm}(E) = d_{\pm}\rho_{\pm}(E) = \sum_{m_1,m_2}^{\prime} I^{m_1,m_2}(E)\,; \quad I^{m_1,m_2}(E) = d(m_1,m_2)\rho^{m_1,m_2}(E)\,. \tag{5.4.4}$$

We employ the Edgeworth (ED) form that includes γ_1 and γ_2 corrections to the Gaussian partial densities $\rho_{\mathscr{G}}^{m_1,m_2}(E)$. Then

$$\rho^{m_1,m_2}(E) \rightarrow \rho_{\mathscr{G}}^{m_1,m_2}(E) \rightarrow \rho_{ED}^{m_1,m_2}(E)$$

and in terms of the standardized variable $\widehat{E}$, the ED form $\eta_{ED}(\widehat{E})$ is given by Eq. (2.3.2). Using Eqs. (5.4.3) and (2.3.2) with exact centroids and variances given by the propagation formulas in Sec. 5.3 and the binary correlation results for γ_1 and γ_2 as given by the formulas in Chapter 7, the smoothed +ve and −ve parity state densities are constructed. We put $\eta_{ED}(\widehat{E}) = 0$ when $\eta_{ED}(\widehat{E}) < 0$. It is clearly seen from Fig. 5.6 that the sum of partial densities, with the partial densities represented by ED corrected Gaussians, describe extremely well the exact fixed-π densities. Therefore, for the (τ,α) values in the range determined by nuclear $sdfp$ and $fpg_{9/2}$ interactions, i.e. $\tau \sim 0.1-0.3$ and $\alpha \sim 0.5\tau - 2\tau$, the partial densities can be well represented by ED corrected Gaussians and total densities are also close to ED corrected Gaussians. Unlike Fig. 5.6, densities in Figs. 5.2, 5.3 and 5.4 show, in many cases, strong departures from Gaussian form. Therefore, it is important to test how well Eq. (5.4.4) with ED corrected Gaussian for $\rho^{m_1,m_2}(E)$ describes the numerical results for $I_{\pm}(E)$. We show this comparison for all the densities in Figs. 5.3 and 5.4. It is clearly seen that the agreements with ED corrected Gaussians are good in all the cases. Therefore, the large deviations from the Gaussian form for $I_{\pm}(E)$ arise mainly because of the distribution of the centroids [this involves dimensions of the (m_1,m_2) configu-

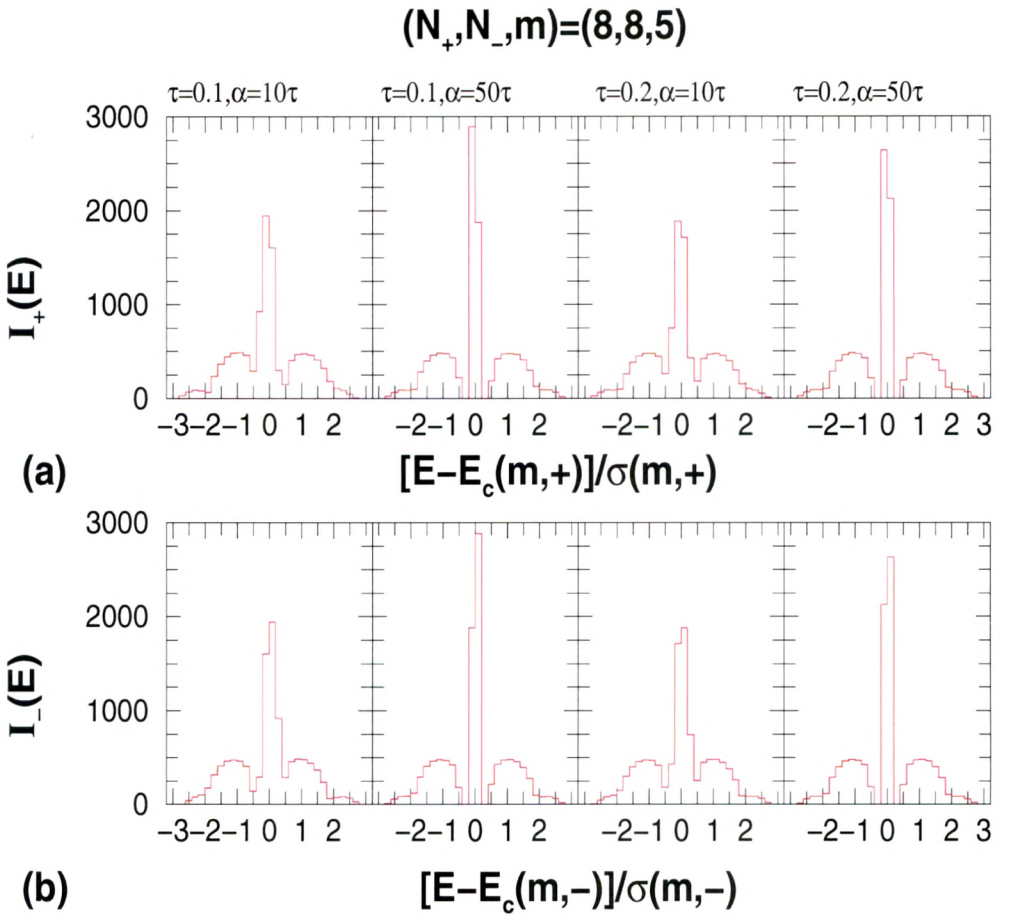

Figure 5.7: (a) Positive and (b) negative parity state densities for some small values of τ and large α values for $(N_+, N_-, m) = (8, 8, 5)$ system. See text for details.

rations] of the partial densities involved. It is possible that the agreements in Figs. 5.3 and 5.4 may become more perfect if we employ, for the partial densities, some non-canonical forms defined by the first four moments as given for example in [Gr-95a, Te-06a]. However, as these forms are not derived using any random matrix ensemble, we haven't used these for the partial densities in our present investigation. In conclusion, for the physically relevant range of (τ, α) values, the propagation formulas for centroids and variances given by Eqs. (5.3.5) and (5.3.6) or alternatively with $E_c(m_1, m_2) = m_2\Delta$ and Eq. (5.3.8) along with the EGOE(1+2)-π ensemble averaged $\gamma_1(m_1, m_2)$ and $\gamma_2(m_1, m_2)$ estimates as given in Chapter 7 can be used to construct fixed-π state densities for larger (N_+, N_-, m) systems. Finally, for a small value of τ but α very large, the densities again become multi-modal and some examples for this are shown in Fig. 5.7. The situation here is similar to the model discussed in [Le-94].

5.4.2 Parity ratios for state densities

As stated in the beginning of this chapter, parity ratio of state densities at a given excitation energy (E) is a quantity of considerable interest in nuclear structure. For the systems shown in Figs. 5.2, 5.3 and 5.4 and also for many other systems, we have studied the parity ratios and the results are shown in Figs. 5.8-5.11. As the parity ratios need to be calculated at a given value of excitation energy E, we measure the eigenvalues in both +ve and −ve parity spaces with respect to the absolute gs energy E_{gs} of the $N = N_+ + N_-$ system. Thus, E_{gs} is defined by taking all the +ve and −ve parity eigenvalues of all members of the ensemble and choosing the lowest of all these. The gs energy can also be determined by averaging the +ve and −ve parity gs energies over the ensemble and then the gs energy is minimum of the two. It is seen that the results for parity ratios are essentially independent of the choice of E_{gs} and thus we employ absolute gs energy in our calculations. We use the ensemble averaged total (+ve and −ve eigenvalues combined) spectrum width σ_t of the system for scaling. The total widths σ_t can be calculated also by using $E_c(m_1, m_2)$ and $\sigma^2(m_1, m_2)$. Examples for σ_t are shown in Table 5.2 and they are in good agreement with the results obtained using the simple formula given by Eq. (5.3.8). We use the variable $\boldsymbol{E} = (E - E_{gs})/\sigma_t$ for calculating parity ratios. Starting with E_{gs} and using a bin-size of $\Delta\boldsymbol{E} = 0.2$, we have calculated the number of states $I_+(\boldsymbol{E})$ with +ve parity and also the number of states $I_-(\boldsymbol{E})$ with −ve parity in a given bin and then the ratio $I_-(\boldsymbol{E})/I_+(\boldsymbol{E})$ is the parity ratio. Note that the results in Figs. 5.8-5.11 are shown for $\boldsymbol{E} = 0 - 3$ as the spectrum span is $\sim 5.5\sigma_t$. To go beyond the middle of the spectrum, for real nuclei, one has to include more sp levels (also a finer splitting of the +ve and −ve parity levels may be needed) and therefore, N_+ and N_- change. Continuing with this, one obtains the Bethe form for nuclear level densities [Ko-10].

General observations from Figs. 5.8-5.11 are as follows. (i) The parity ratio $I_-(\boldsymbol{E})/I_+(\boldsymbol{E})$ will be zero up to an energy $\boldsymbol{E}_0$. (ii) Then, it starts increasing and becomes larger than unity at an energy $\boldsymbol{E}_m$. (iii) From here on, the parity ratio decreases and saturates quickly to unity from an energy $\boldsymbol{E}_1$. In these examples, $\boldsymbol{E}_0 \lesssim 0.4$, $\boldsymbol{E}_m \sim 1$ and $\boldsymbol{E}_1 \sim 1.5$. It is seen that the curves shift towards left as τ increases. Also the position of the peak shifts to much larger value of $\boldsymbol{E}_m$ and equilibration gets delayed as

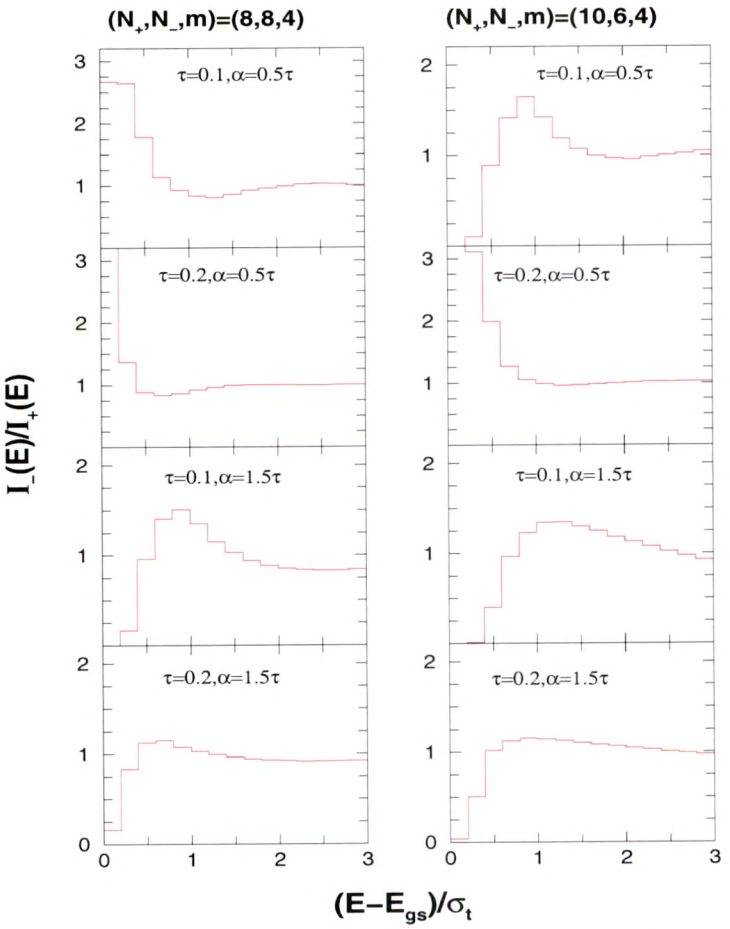

Figure 5.8: Parity ratios for various (τ, α) values for $(N_+, N_-, m) = (8,8,4)$ and $(10,6,4)$ systems. See text for details.

α increases for a fixed τ value. Therefore for larger τ, the energies $(\boldsymbol{E}_0, \boldsymbol{E}_m, \boldsymbol{E}_1)$ are smaller compared to those for a smaller τ. The three transition energies also depend on (N_+, N_-, m). We have also verified, as shown in Fig. 5.10, that the general structure of the parity ratios will remain same even when we change $\Delta \rightarrow -\Delta$ (i.e., $-$ve parity sp states below the +ve parity sp states). For $(N_+, N_-, m) = (8,8,4)$ system, results for $\Delta = 1$ are given in Fig. 5.8 and they are almost same as the results with $\Delta = -1$ given in Fig. 5.10. The general structures (i)-(iii) are clearly seen in the numerical examples shown in [Mo-07] where a method based on the Fermi-gas model has been employed. If $\sigma_t \sim 6-8$ MeV, equilibration in parities is expected around $E \sim 8-10$ MeV and this is clearly seen in the examples in [Mo-07]. It is also seen from Fig. 5.9 that equilibration is quite poor for very small values of τ and therefore comparing with the results in [Mo-07], it can be argued that very small values of τ are ruled out

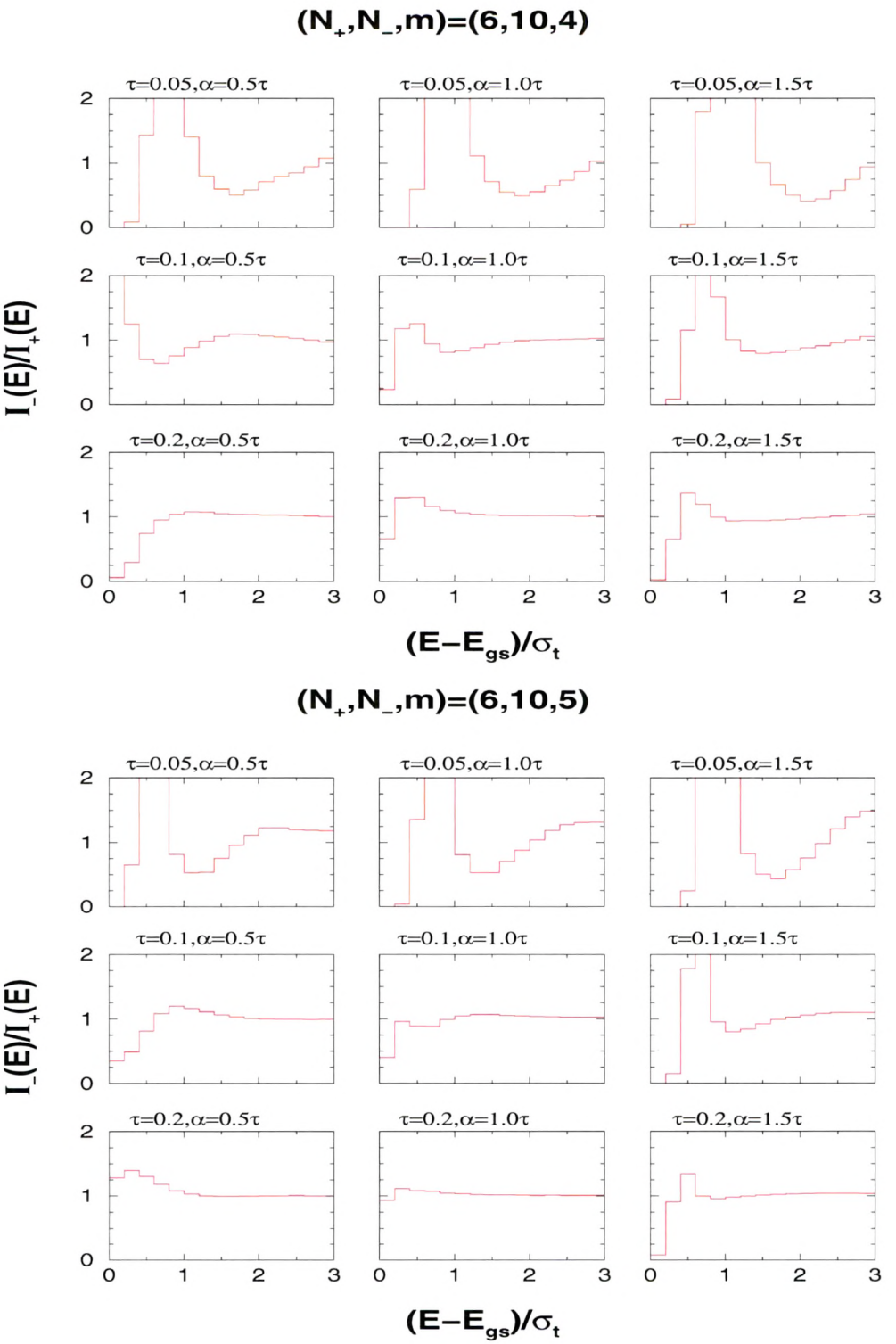

Figure 5.9: Parity ratios for various (τ, α) values for $(N_+, N_-, m) = (6, 10, 4)$ and $(6, 10, 5)$ systems. See text for details.

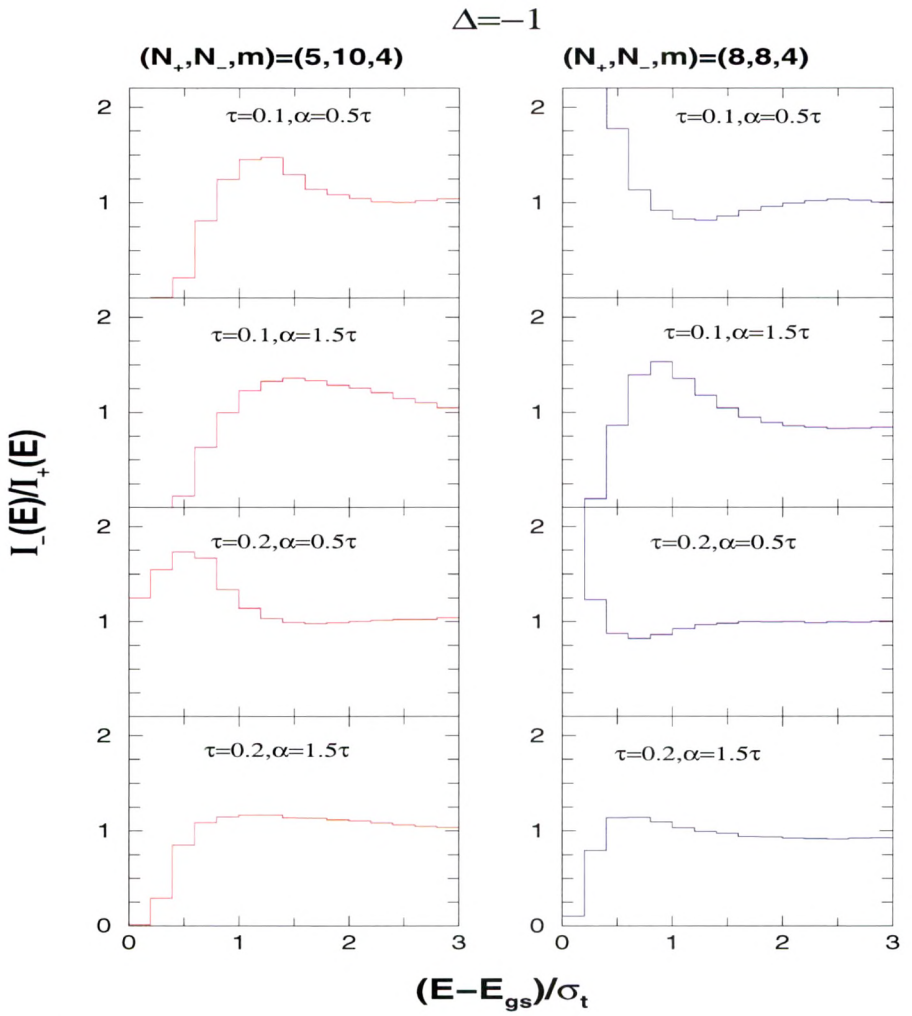

Figure 5.10: Parity ratios for some values of (τ, α) with $\Delta = -1$ for $(N_+, N_-, m) = (5, 10, 4)$ and $(8, 8, 4)$ systems. See text for details.

for nuclei. Hence, it is plausible to conclude that generic results for parity ratios can be derived using EGOE(1+2)-π with reasonably large (τ, α) values. Let us add that the interpretations in [Mo-07] are based on the occupancies of the sp orbits while in the present chapter, they are in terms of τ and α parameters.

Using the smoothed $I_{\pm}(\boldsymbol{E})$, constructed as discussed in Sec. 5.4.1, smoothed forms for parity ratios are calculated as follows. Starting with the absolute gs energy E_{gs} and using a bin-size of $\Delta\boldsymbol{E} = 0.2$, +ve and −ve parity densities in a given energy bin are obtained and their ratio is the parity ratio at a given $\boldsymbol{E}$. We have chosen the examples where I_+ and I_- are close to Gaussians. It is seen from Fig. 5.11 that the agreement with exact results is good for $\boldsymbol{E} \gtrsim 0.5$. However, for smaller $\boldsymbol{E}$, to obtain a

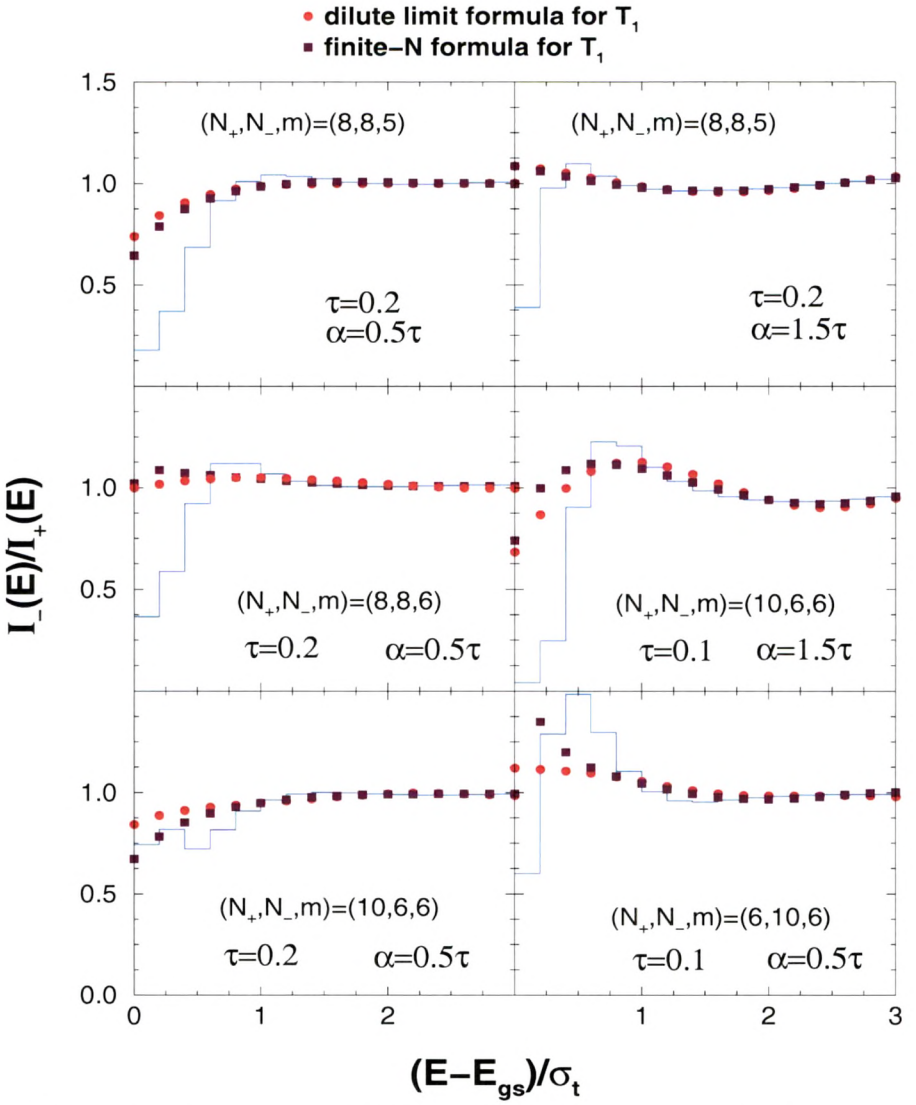

Figure 5.11: Parity ratios for various (τ, α) values and for various (N_+, N_-, m) systems. Filled circles (red) and squares (brown) are obtained using fixed-(m_1, m_2) partial densities with dilute limit formula and finite-N formula for the functions $F(\cdots)$ given in Eqs. (H14) and (H23) respectively that are required to calculate T_1 in Eq. (7.2.8); see Chapter 7 and Appendix H for details.

good agreement one should have a better prescription for determining the tail part of the $\rho^{m_1,m_2}(\boldsymbol{E})$ distributions. Developing the theory for this is beyond the scope of the present thesis as this requires more complete analytical treatment of the ensemble.

5.4.3 Probability for +ve parity ground states

Papenbrock and Weidenmüller used the $\tau \to \infty$, $\alpha = \tau$ limit of EGOE(1+2)-π for several (N_+, N_-, m) systems to study the probability (R_+) for +ve parity ground states

over the ensemble [Pa-08]. As stated before, this exercise was motivated by shell-model results with random interaction giving preponderance of +ve parity ground states [Zh-04]. The numerical calculations in [Pa-08] showed considerable variation $(18-84\%)$ in R_+. In addition, they gave a plausible proof that in the dilute limit $[m << (N_+, N_-)]$, R_+ will approach 50%. Combining these, they argued that the observed preponderance of +ve parity ground states could be a finite size (finite N_+, N_-, m) effect. For the extended EGOE(1+2)-π considered in the present chapter, where the $\tau \to \infty$ and $\alpha = \tau$ restriction is relaxed, as we will discuss now, R_+ can reach 100%.

For EGOE(1+2)-π with $\tau \sim 0$, clearly one will get $R_+ = 100\%$ (for even m and $m << N_+, N_-$) and therefore it is of interest to study R_+ variation with (τ, α). We have carried out calculations using a 200 member ensemble for $(N_+, N_-, m) = (6,6,6)$ and 100 member ensembles for $(8,8,5)$, $(6,6,6)$, $(6,10,4)$ and $(6,10,5)$ systems. In these calculations, we use $\alpha = \tau$ and 1.5τ. The results are shown in Fig. 5.12. For $\alpha = \tau$, the results are as follows. For $\tau \lesssim 0.04$, we have $R_+ \sim 100\%$ and then R_+ starts decreasing with some fluctuations between $\tau = 0.1$ and 0.2. The origin of these fluctuations is not clear. As $\tau > 1$ is not realistic, we have restricted the R_+ calculations to $\tau \leq 1$. We see from the figure that EGOE(1+2)-π generates $R_+ \gtrsim 50\%$ for $\tau \leq 0.3$ independent of (N_+, N_-, m). Also, R_+ decreases much faster with τ and reaches $\sim 30\%$ for $\tau = 0.5$ for $(N_+, N_-, m) = (6,6,6)$. For $m < (N_+, N_-)$, the decrease in R_+ is slower. If we increase α, from the structure of the two-particle H matrix in Fig. 5.1, we can easily infer that the width of the lowest +ve parity (m_1, m_2) unitary configuration becomes much larger compared to the lowest $-$ve parity unitary configuration (see Table 5.2 for examples). Therefore, with increasing α we expect R_+ to increase and this is clearly seen in Fig. 5.12. Thus $\alpha \gtrsim \tau$ is required for R_+ to be large. A quantitative description of R_+ requires the construction of +ve and $-$ve parity state densities more accurately in the tail region and the theory for this is not yet available.

5.5 Summary

In the present chapter, we have introduced a generalized EGOE(1+2)-π ensemble for identical fermions and its construction follows from EGOE(1+2) for spinless fermion systems. Using this generalized EE, we have not only studied R_+, as it was done by Papenbrock and Weidenmüller [Pa-08] using a simpler two-body ensemble with par-

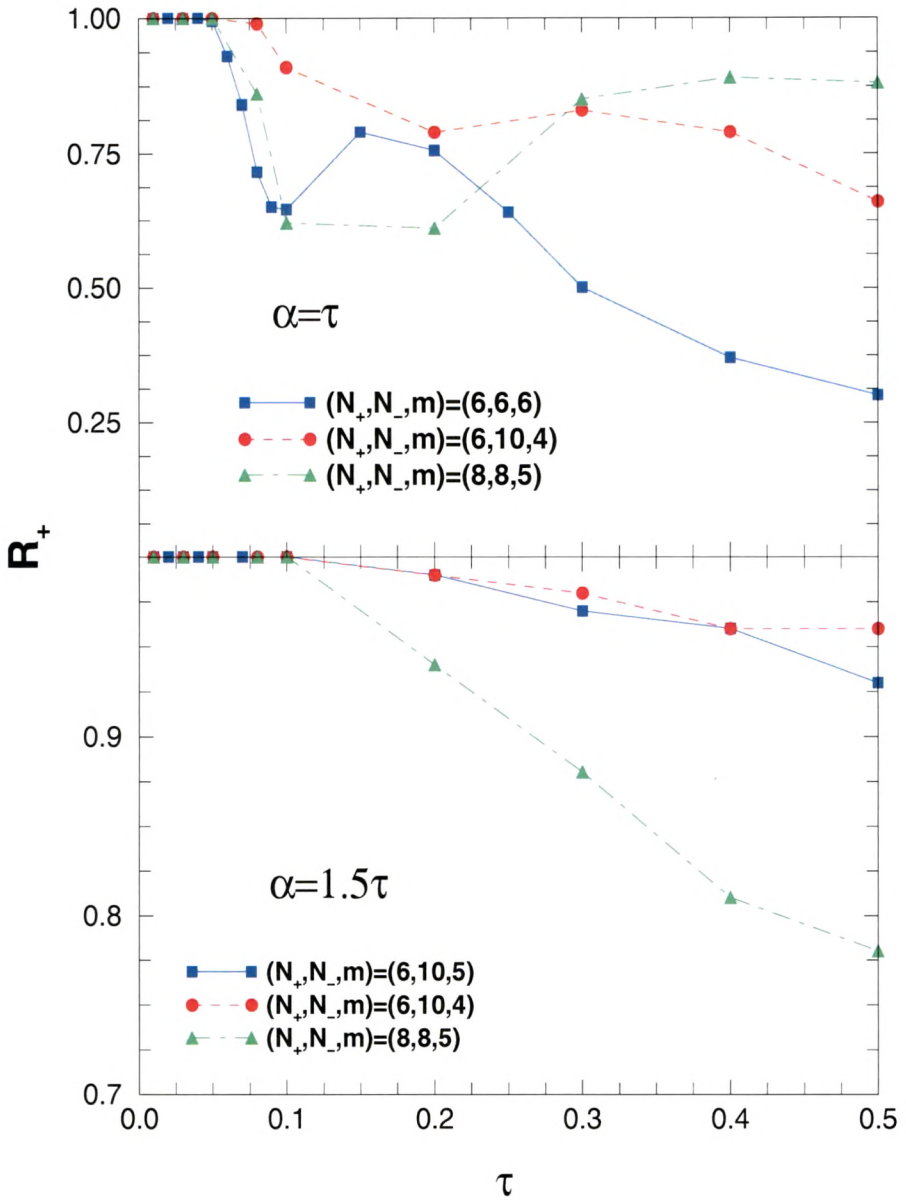

Figure 5.12: Probability (R_+) for +ve parity ground states for various (τ, α) values and for various (N_+, N_-, m) systems. See text for details.

ity, but also studied the form of fixed-π state densities and parity ratios which are important nuclear structure quantities. Numerical examples (see Figs. 5.2-5.4 and 5.6), with the range of the various parameters in the model fixed using realistic nuclear effective interactions, are used to show that the fixed-π state densities in finite dimensional spaces are of Gaussian form for sufficiently large values of the mixing parameters (τ, α). The random matrix model also captures the essential features of parity ratios as seen in the method based on non-interacting Fermi-gas model reported

in [Mo-07]. We also found preponderance of +ve parity ground states for $\tau \lesssim 0.5$ and $\alpha \sim 1.5\tau$. In addition, for constructing fixed-π Gaussian densities we have derived an easy to understand propagation formula [see Eq. (5.3.6)] for the spectral variances of the partial densities $\rho^{m_1,m_2}(E)$ that generate I_+ and I_-. Similarly, for calculating the corrections to the Gaussian forms, formulas for skewness γ_1 and excess γ_2 of the partial densities $\rho^{m_1,m_2}(E)$ are derived using the binary correlation approximation (see Chapter 7 for the formulas). The smoothed densities constructed using Edgeworth corrected Gaussians are shown to describe the numerical results for $I_\pm(E)$ [for (τ, α) values in the range defined by nuclear $sdfp$ and $fpg_{9/2}$ interactions - see beginning of Sec. 5.4] and also the parity ratios at energies away from the gs. Numerical results presented for parity ratios at lower energies show that a better theory for the tails of the partial densities is needed (see Figs. 5.8-5.11). Thus, the results in the present chapter represent considerable progress in analyzing EGOE(1+2)-π ensemble going much beyond the analysis presented in [Pa-08].